Preprints.org

Article

Not peer-reviewed version

Water Balance Driven by Land Use and Land Cover Change across the Amazon Basin

Celso Bandeira de Melo Ribeiro *, Binayak Mohanty, Otto Corrêa Rotunno Filho, Eduarda Trindade Filgueiras, Luciano Nóbrega Rodrigues Xavier, Afonso Augusto Magalhães de Araujo

Posted Date: 9 October 2023

doi: 10.20944/preprints202310.0383.v1

Keywords: water cycle; Amazon basin; deforestation

Preprints.org is a free multidiscipline platform providing preprint service that is dedicated to making early versions of research outputs permanently available and citable. Preprints posted at Preprints.org appear in Web of Science, Crossref, Google Scholar, Scilit, Europe PMC.

Copyright: This is an open access article distributed under the Creative Commons Attribution License which permits unrestricted use, distribution, and reproduction in any medium, provided the original work is properly cited.

Preprints (www.preprints.org) | NOT PEER-REVIEWED | Posted: 9 October 2023 doi:10.20944/preprints202310.0383.v1

Disclaimer/Publisher's Note: The statements, opinions, and data contained in all publications are solely those of the individual author(s) and contributor(s) and not of MDPI and/or the editor(s). MDPI and/or the editor(s) disclaim responsibility for any injury to people or property resulting from any ideas, methods, instructions, or products referred to in the content.

Article

Water Balance Driven by Land Use and Land Cover Change across the Amazon Basin

Celso Ribeiro [1,‡,*], Binayak Mohanty [2,‡], Otto Corrêa Rotunno Filho [3,‡], Eduarda Filgueiras [1,‡], Luciano Xavier [4,‡] and Afonso Araújo [5,‡]

1 Department of Sanitation and Environmental Engineering, Federal University of Juiz de Fora (UFJF), Juiz de Fora (MG) – Brazil
2 Department of Biological and Agricultural Engineering, Texas A&M University, College Station, Texas, USA
3 Water Resources and Environmental Studies Laboratory (LABH2O), Civil Engineering Program, Alberto Luiz Coimbra Institute for Graduate School and Research in Engineering (COPPE), Federal University of Rio de Janeiro (UFRJ), Rio de Janeiro (RJ) – Brazil
4 Electric Energy Research Center (CEPEL), Campus Ilha do Fundão, Rio de Janeiro (RJ) – Brazil
5 Department of Water Resources and Environmental Studies, Politechnical School of Engineering, Federal University of Rio de Janeiro (UFRJ), Rio de Janeiro (RJ) – Brazil
* Correspondence: celso.bandeira@ufjf.br
‡ These authors contributed equally to this work.

Abstract: Despite the overall extension of the Amazon basin (approximately $6,000,000\,km^2$),which encompasses such a complex ecosystem and territories belonging to seven different nations, it is worth mentioning that environmental assessment related to changes in land use and land cover (LULC) in this region are often conducted respecting geopolitical boundaries associated with each country or taking into account the so-called Amazon biome. With the purpose of prospecting the intricate and hidden hydrological patterns, we undertake an in-depth evaluation of the water balance along the 2001-2021 time span across the whole basin, whose behavior depends on the features deriving from the metamorphoses in land use and land cover. To accomplish that task, the influence of the components of the water balance, namely rainfall and evapotranspiration, jointly with the terrestrial topographic mapping, are examined to investigate the interactions among the physical mechanisms that make up the hydrological cycle and the corresponding physical hydrological processes triggered by deforestation and reforestation in the region. More specifically, the modeling approach was rigorously designed to also consider, separately or not Negro, Solimões, Madeira, Tapajós and Xingu hydrographic sub-basins, which are the most important ones of the Amazon basin. The results highlight that, in the southern region of the Amazon, specifically within the Madeira river sub-basin, the lowest forest coverage is observed (56.0%), whereas in the northern Negro river sub-basin, the most notable forest coverage is observed (85.0%).The most preserved forest areas, such as the Negro and Solimões river sub-basins, with percentages of 81.9% and 74.2%, respectively, have higher annual rates of precipitation and evapotranspiration over time. On the other hand, regions that suffered the most intense deforestation along the time period studied, such as the Madeira, Tapajós and Xingu sub-basins, have lower annual rates of precipitation and evapotranspiration, with a preservation percentage of 54.6%, 62.6% and 70, 7%, respectively. As the pace of deforestation slowed between 2003 and 2013, annual precipitation rates increased by 12.0%, while evapotranspiration decreased by 2.0%. The hydrological findings of this paper highlight th predominant role of the forest in the context of the global water balance of the Amazon basin and the potential to also produce distinct impacts within different parts of the basin in terms of having more or less rainfall and evaporation. In addition, those variabilities in the hydrological operational components and mechanisms due to changes in land cover and land use also reveals the potential impacts that could be expected in the surrounding areas, closer or farther, notably beyond the limits of the Amazon basin.

Keywords: water cycle; Amazon basin; deforestation

© 2023 by the author(s). Distributed under a Creative Commons CC BY license.

Preprints (www.preprints.org) | NOT PEER-REVIEWED | Posted: 9 October 2023 doi:10.20944/preprints202310.0383.v1

1. Introduction

The Amazon basin is recognized to be the largest watershed on the planet [1] covering about $6,000,000\,km^2$ comprising about a third of the South American continent and one third of the world's rainforests. The region has also the most extensive drainage network of the globe, contributing approximately 20 % of the total river flow on the planet.

In addition, the biomass [2,3] of the Amazon basin amounts to approximately 100 billion tons of carbon, which corresponds to more than 10 years of issuance of fossil fuels [4]. This watershed has aroused great interest in the scientific community and with respect to the world public opinion due to LULC change [5,6] impacts on ecosystem services [7,8] provided by its rainforest, including the corresponding water balance and energy balance [9,10], biodiversity [11], climate regulation [12,13], carbon storage [14,15] and water supply for the Brazilian power sector [16,17]. The understanding of processes controlled by its forest cover at the local, regional and global level is currently among the major environmental challenges for life on Earth.

Previous studies have shown trends of changes in forest cover worldwide and the importance of Amazon Basin in this aspect, which shares 32% of global coverage of tropical forest in the world [18]. It is well known that the biggest problem facing this region comes from deforestation [19], mainly due to socioeconomical issues [20]. The Brazilian National Institute for Space Research (INPE) periodically quantifiesy the deforestation levels in the Amazon region. However, the approach proposed therein pursues the estimation of the annual deforestation rates since 1988 within the limits of the Brazilian Legal Amazon, disregarding other countries covered by the basin such as Peru, Ecuador, Bolivia, Colombia, Venezuela and Guyana, which together account for about 37% of its area.

Complementarily, it should be noted that a relative recent study claimed that there is a direct relationship between rainfall abundance in the Amazon region with the preserved forest presence [21]. In this process, moisture coming from the ocean ("blue sea") plus the evapotranspiration ("green sea") is combined to form hygroscopic nuclei, [22], causing large amount of precipitation in the region.

Thus further investigations should be conducted to address the LULC changes in Amazon basin under a framework of detailed spatial-temporal analysis, not only considering the entire basin but also aiming at identifying the hydrometeorological patterns in its primary subbasins (Solimões, Madeira, Negro, Tapajós and Xingu). since each one of these subbasins has been subjected to varying degrees of change over the last decades, it seems that these differences should be properly taken into account allow a deeper comprehension of the resulting impacts in terms of water and energy balances at the basin scale.

This study proposes to enhance the comprehension of the overall basin behaviour emphasizing the important of exploring such worldwide crucial region for the planet at the sub-basin scale by examining LULC changes in the Amazon basin during the 2001-2021 time period. Moreover reainfall and evapotranspiration patterns are revealed, while irrigation pratices are also examined along the adopted time frame.

Remotely sensed products for precipitation and evapotranspiration, namely MODIS (Moderate Resolution Imaging Spectroradiometer)(MOD16)and CHIRPS (Climate Hazards Group Infrared Precipitation with Station), respectively, were used [24] in the analysis. The paper is structured in five sections: (i) Section 1 presents the reason-why of the development of the research work pointing out some gaps in the literature so far published; (ii) Section 2 introduces the datasets employed within a proposed work flow for the development of the methodological approach adopted; (iii) Section 3 presents results and analysis; (iv) Section 4 presents further discussions and reflection with respect to the results presented; (v) Section 5 presents concluding remarks for the manuscript.

Such type of constraints and motivations highlighted in previous published revised literature foster further investigations to address the LULC changes in Amazon basin under a detailed spatio-temporal framework, not only considering the entire basin, but also aiming at identifying the hydrometeorological patterns in its primary subbasins (Solimões, Madeira, Negro, Tapajós and Xingu).

Preprints (www.preprints.org) | NOT PEER-REVIEWED | Posted: 9 October 2023 doi:10.20944/preprints202310.0383.v1

2. Materials and Methods

Landscape evolution and associated changes in LULC due to human occupation, in special regarding deforestation and forest regeneration, jointly the water and energy balances in the Amazon basin require increasing attention. Such endeavors to develop state-of-the-art research topics in the recent decades over this area deserves to be recognized. . In this sense, the paper focused to examine more closely the 2001-2021 time span. A comprehensive analysis of the interrelationships between precipitation (P) and evapotranspiration (ET) is developed for the Amazon region, considering sociopolitical factors and diversity of ecosystemic influences.

To conduct the investigation, remote sensing data obtained from several satellites were used to perform the proposed analysis. Such approach allowed for detailed assessments in each of the five main subbasins of the Amazon basin, formed by the subbasins of the Negro, Solimões, Madeira, Tapajós and Xingu rivers. As previously stated, the study not only analyzed the water balance of the entire basin, but also examined its relationship with LULC in different portion of the region. Along this section, the procedures used to obtain spatial and temporal data for the P and ET variables, as well as LULC data, for the Amazon basin are briefly exposed and commente. The referred set of procedures provided a robust basis for the analysis and interpretation of weather patterns and the impacts of human activities in the Amazon basin. The Figure 1 presents the schematic flowchart of the methodology addopted for the present study.

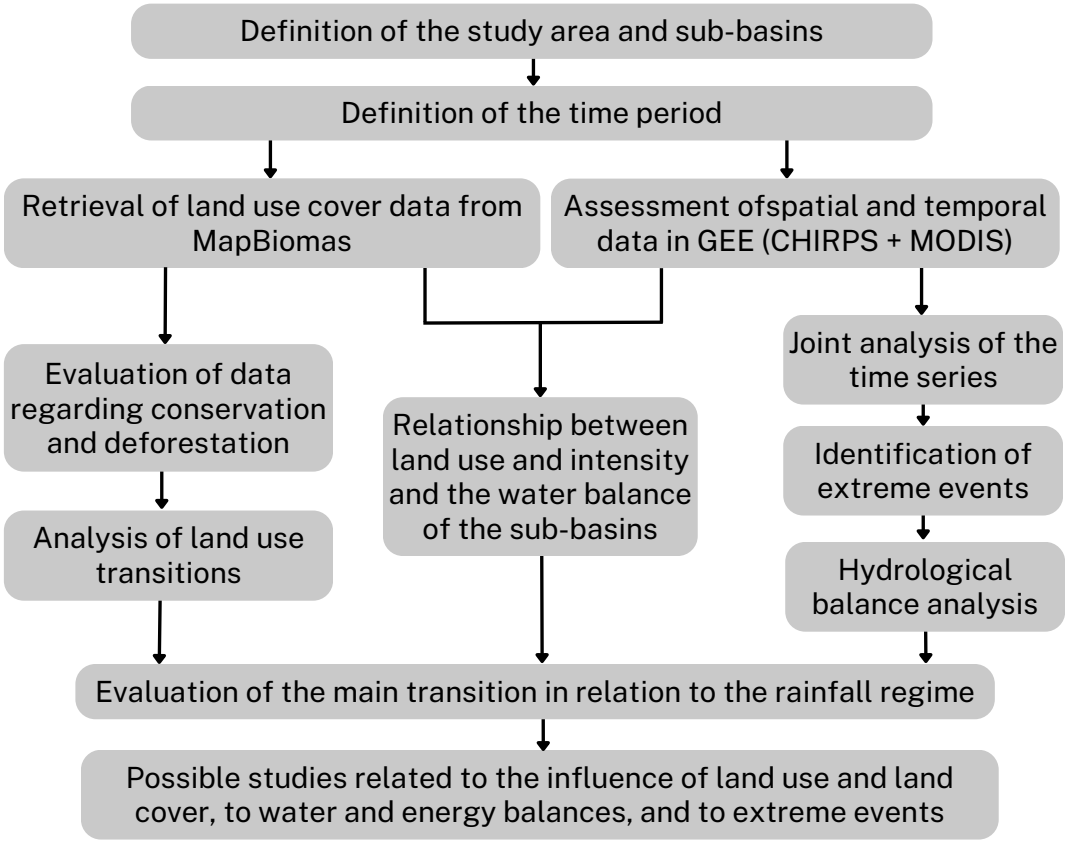

Figure 1. Schematic representation of the work flow for the applied methodology.

2.1. Study area

The selection of the Amazon Basin as the focus of this study stems from its profound significance in providing environmental services at local, regional, and global scales. The basin is globally recognized for its rich biodiversity and abundant water resources.

Spanning approximately 6.1 million square kilometers, the Amazon Basin constitutes the Earth's most expansive hydrographic network. Encompassing about 30% of the landmass of South America, it

Preprints (www.preprints.org) | NOT PEER-REVIEWED | Posted: 9 October 2023 doi:10.20944/preprints202310.0383.v1

extends from its sources in the Peruvian Andes to its mouth at the Atlantic Ocean in northern Brazil, traversing territories of Brazil, Colombia, Bolivia, Ecuador, Guyana, Peru, and Venezuela [1].

The Figure 2 illustrates the Amazon basin and it's position in within the South American continent, outlining its geographical location and the main watercourses comprising its extensive hydrographic network, including its significant sub-basins.

Over the past three decades, the accelerated LULC in this basin has been primarily driven by timber extraction, agriculture, livestock, and mining, underscoring the urgent need to establish a socioeconomic development model that allows for the rational exploitation of its natural resources while safeguarding its crucial provision of global-scale environmental services.

The intense deforestation witnessed in this basin in recent decades has garnered global attention, prompting a comprehensive exploration of the resulting impacts on LULC, hydrological balance, energy dynamics, and climatology. Such situation holds fundamental importance both in the scientific and societal domains and deserves to be more profoundly evaluated.

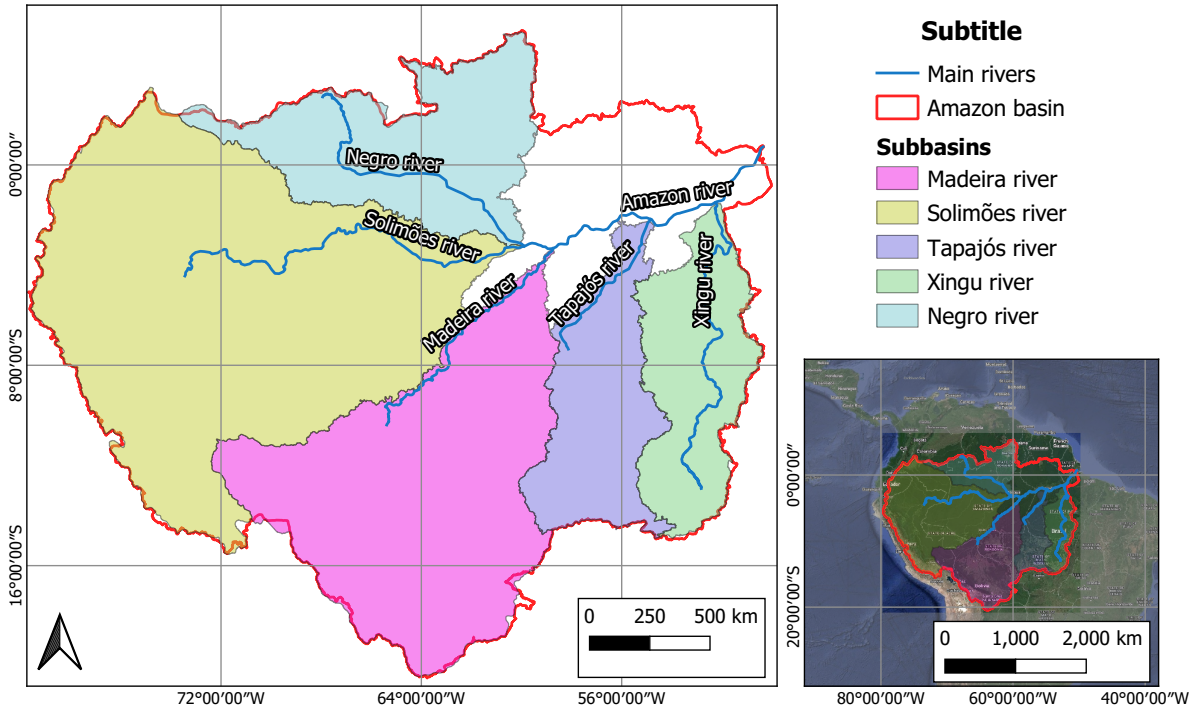

Figure 2. Location and main sub-basins that make up the Amazon basin.

2.2. Land use and land cover changes

The spatio-temporal analysis of LULC for the entire Amazon basin was carried out using LULC data provided by the MapBiomas project [1] as an important basis for a comprehensive analysis of deforestation, reforestation, and their impact on the water and energy balances in the Amazon basin. MapBiomas provides detailed information about changes in vegetation cover over time, allowing for the accurate identification and monitoring of environmental changes. For the case study region, these vegetation classes represent 89 to 99% of the area, with the remainder covered by water (rivers, floodplains, and lakes).

[1] Based on Landsat mosaics, classifications are obtained, resulting in thematic maps of LULC for each year. Following the logical approach proposed by MapBiomas Amazonia, the maps are updated whenever there is an improvement in classification algorithms. The classification methodology is dynamic, aiming to refine the classification of each typology. Available at: https://urx1.com/dEKEi.

Preprints (www.preprints.org) | NOT PEER-REVIEWED | Posted: 9 October 2023 doi:10.20944/preprints202310.0383.v1

The complete MapBiomas 4 Collection used in this study covers a period of 37 years, from 1985 to 2021, which represents a extended time period in comparison to the 2001/2021 time span used in-here.This MapBiomas Collection provides detailed information on the dynamic of forest areas, cerrados, urban areas, agriculture, pastures and other LULC. Such data allow for a comprehensive and reliable analysis of the transformations that have occurred over time.

The methodological approach was designed to highlight the effects of LULC by relating P and ET in the hydrological cycle of the Amazon basin. A detailed assessment of the different sub-basins that constitute the entire system was conducted, providing support to better analyze the implications at local and remote areas for both small and large-scale circulation mechanisms, given the importance of the region on a global scale. The proportion of LULC in the Amazon basin for 2001 and 2021, separately is presented in Figure 3. It should be noted that Landsat images were used to represent the entire area of the Amazon basin for each of the 21 years during the study period.

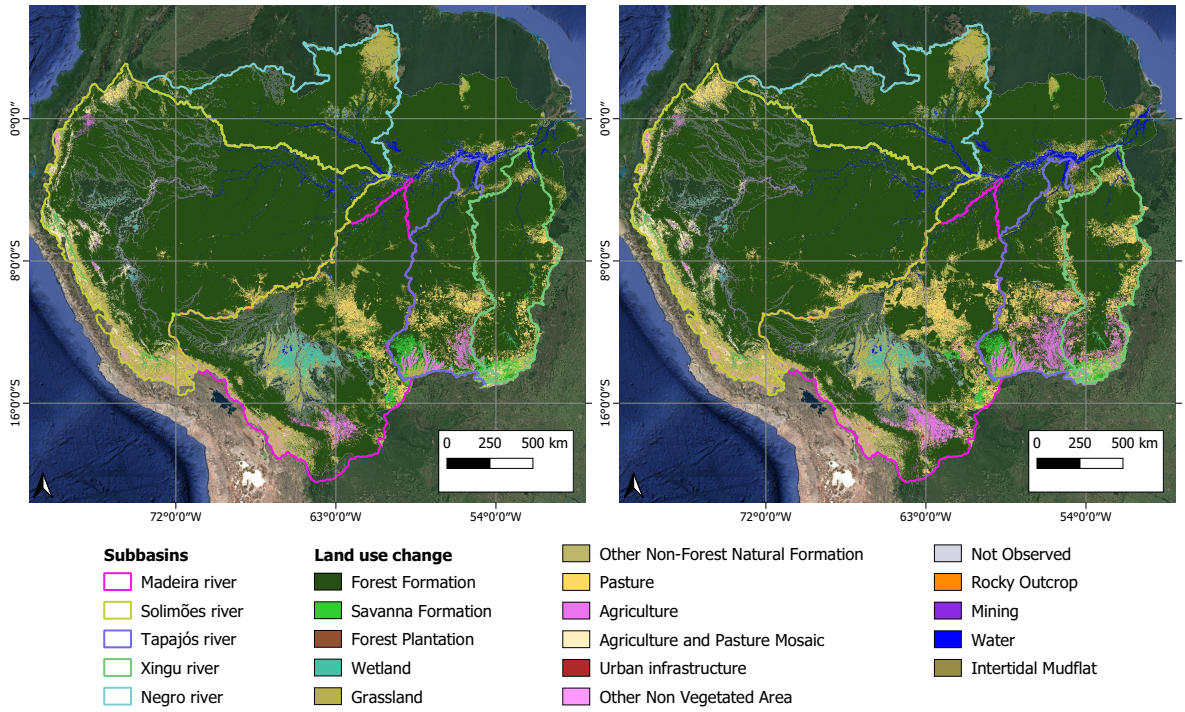

Figure 3. Land use and land cover changes within the borders of the Amazon basin based on classification procedures adopted by MapBiomas: a) 2001 (on the left) and b) 2021 (on the right).

2.3. Spatial distribution of P and ET

The P and ET data are essential for analyzing the water balance of the basin. For this purpose, the Google Earth Engine (GEE) platform of geospatial analysis was used, which allows the visualization and analysis of satellite images of the entire planet, to obtain and accumulate monthly P and ET data referring to the period from 2001 to 2021, by creating a programming code [2].

The monthly spatial and temporal distribution of P across the Amazon basin was obtained using the CHIRPS dataset [3]. The historical series was obtained using Algorithm A1 (Appendix A). The algorithm developed at GEE aims to analyze P data in the Amazon basin. First, the watershed

[2] The programming code in GEE is based on JavaScript, a high-level, interpreted, object-oriented programming language.
[3] The Climate Hazards Group InfraRed Precipitation with Stations is a dataset with a spatial resolution of 5 km and geographic coverage of 50ºS to 50ºN . It contains weather information from 1981 to the present day, including daily, 5-day and monthly data.

Preprints (www.preprints.org) | NOT PEER-REVIEWED | Posted: 9 October 2023 doi:10.20944/preprints202310.0383.v1

boundaries are added and an empty image is created to delineate its contour. Next, a range of years and a list of months are defined for the period of interest.

Using the P CHIRPS image collection, images covering the basin area are selected within the desired time period. In the next step, the filtered images for each month and year are added, generating the monthly accumulated P for analysis. The results are presented by means of an interactive time series graph, showing the average monthly P accumulated over time in the Amazon basin.

On the other side, the ET data distribution was obtained using the MOD16A2 Version 6 dataset[4]. For the subbasins of the Amazon basin, historical series data from 2001 to 2021 were acquired.

The temporal distribution of the ET data was extracted from Algorithm A2 (Appendix A), which performs a monthly cumulative ET analysis for the Amazon basin using data from the MODIS product. Initially, a collection of features representing the boundaries of the Amazon basin is loaded. Next, an empty image is created, and, on this image, the contour of the watershed is drawn. A range of years is generated, and two dates (beginning year and final year) are created to filter the MODIS image collection, selecting only ET images within the specified period and within the area of interest. The code calculates the cumulative monthly evapotranspiration for each month and year within the defined range. The calculations involve filtering the MODIS images for each month and year, followed by summing the images to obtain the accumulated monthly evapotranspiration.

2.4. Temporal distribution of P and ET

To obtain the spatial distribution of P, Algorithm A3 (Appendix B) was used. The GEE code performs the analysis of the monthly average P in the Amazon basin, using data from the CHIRPS product. First, a collection of features representing the boundaries of the Amazon basin is loaded. Following, the desired start and end years of interest are selected, together with the number of the desired month for the analysis.

Based on the defined parameters, a range of years is created, and the collection of CHIRPS images is filtered according to the specified area and time period. The algorithm implements the `calculatePMonth` function to estimate the average monthly P for each year and month within the chosen range. Next, a collection of images is created containing the average monthly P for the selected month.

The minimum and maximum P values are obtained for the analyzed month, which will be used to normalize the P data in a predefined color scale. The normalized values are then visualized on a map using a specific color palette.

The Algorithm A4 (Appendix B) in the GEE code presented here-in performs the analysis of the average monthly ET for the Amazon basin using MODIS data. First, a collection of features representing the boundaries of the Amazon Basin is loaded. Next, the beginning and final years of interest are defined, as well as the desired month for analysis. Based on the defined parameters, a range of years is created, and the MODIS image collection is filtered according to the specified area and time period. The selection is performed considering only the ET variable.

The algorithm implements the `calculateETMonth`function to calculate the average monthly ET for each year and month within the specified range. Calculations are performed by summing the filtered MODIS images for each month and year, which are then multiplied by 0.1 to obtain the ET value in appropriate units. An image collection containing the average monthly ET is created based on the calculation results. The minimum and maximum ET values of the analyzed month are obtained, which will be used to normalize the data in a predefined color scale. Normalized values are visualized on a map with a specific color palette. Finally, a legend is defined for the layer added to the

[4] The Moderate Resolution Imaging Spectroradiometer MOD16A2 Version 6 Evapotranspiration/Latent Heat Flux product is an 8-day dataset with a spatial resolution of 500 meters. The algorithm used is based on the Penman-Monteith equation and incorporates data from daily meteorological reanalysis, as well as remote sensing data products.

Preprints (www.preprints.org) | NOT PEER-REVIEWED | Posted: 9 October 2023 doi:10.20944/preprints202310.0383.v1

map, representing the average ET of the selected month in the Amazon basin region. The algorithm allows a visual representation of the average monthly ET in the Amazon basin region, providing important information about ET patterns over the study period. This visualization allows for a better understanding of variations in ET across the Amazon Basin, contributing to valuable insights into the hydrological processes and dynamics of the region's ecosystems.

3. Results

3.1. Soil cover in the Amazon subbasins

The subbasins of the Negro, Solimões, Madeira, Tapajós and Xingu rivers emerge as the main focal points within the extensive Amazon basin. Therefore, to understand the dynamics and implications of changes in LULC over time, it is imperative to classify these aspects systematically.

In the first approach to depict some of the classification results, Table 1, shows LULC classesjust for the years 2001 and 2021 and their corresponding differences. Moreover, the analysis of the outlined differences becomes fundamental for understanding the evolution of LULC patterns over 2001-2021 time span. Such an analysis reveals a panoramic perspective of the metamorphoses that have indelibly marked this crucial region over two decades. It is important to highlight that values classified as "Not Observed" are missing data from the data set.

Upon examining the highest values, an unmistakable pattern materializes, that is, the forest formation reigning supreme in the Table 1, involving 75.96 % and 71.54 % of the aggregate extension in 2001 and 2021, respectively. This enduring prevalence of the Amazon rainforest underscores its deep and enduring presence.

On the other hand, Table 1 highlights increase in LULC. . For instance, pasture and agriculture categories grew by 2.10 % (126, 256 km^2) and 1.41 % (84, 718 km^2), respectively. Such increase suggests a deliberate expansion of land allocated to these referred activities during the analyzed period, likely a byproduct of human interventions.

Simultaneously, certain variations take a path of moderation. The agricultural and pastures mosaic category exhibits a measured increase of 0.36 %, while the grassland class features a subtle change of 0.19 %.

However, a subset of categories plays a moderate role in the land cover composition scheme. Rocky outcrops, intertidal mudflats, and other non-vegetated area contribute modestly, each with a presence of less than 1 % in both instances, symbolizing their peripheral impact on the overall landscape dynamics.

Nevertheless, a notable phenomenon resides in the context of negative values, serving as a portentous indicator of land cover reduction in specific categories over two decades. It is within these negative trends that the narrative of profound landscapes unfolds, shedding light on the inherently dynamic nature of LULC.

The forest formation category emerges as a focal point of significance, with a delta of -4.42 % ($-265, 162$ km^2). Furthermore, this substantial decrease underlines a distinct reduction in forest cover across the geographic range during the designated interval.

Similarly, the classifications for savanna formation and wetlands reveal negative deviations of -0.16 % and -0.20 %, respectively. These variations might indicate disruptions within these ecosystems, unveiling a narrative of shifts towards alternative usage paradigms, which bear witness to the gradual decline of these environments throughout the course of thise analysis.

Preprints (www.preprints.org) | NOT PEER-REVIEWED | Posted: 9 October 2023 doi:10.20944/preprints202310.0383.v1

Table 1. Percentage of ground cover in the Amazon basin in 2001 and 2021.

LULC Classes	2001 (%)	2021 (%)	Dif. (%)
Pasture	4.37	6.48	2.10
Agriculture	1.10	2.51	1.41
Not Observed	5.63	6.07	0.44
Agriculture and Pasture Mosaic	1.50	1.87	0.36
Grassland	5.62	5.81	0.19
Other Non-Forest Natural Formation	0.83	0.86	0.02
Water	1.81	1.87	0.07
Planted Forest	0.01	0.05	0.04
Mining	0.02	0.05	0.03
Urban infrastructure	0.05	0.08	0.03
Other Non-Vegetated Area	0.39	0.46	0.07
Rocky Outcrop	0.01	0.01	0.00
Intertidal Mudflat	0.01	0.01	0.00
Savanna Formation	1.29	1.13	-0.16
Wetland	1.39	1.19	-0.20
Forest Formation	75.96	71.54	-4.42

The analysis conducted from 2001 to 2021 revealed that, despite all the mentioned subbasins showing a significant loss of forest cover, the Negro River basin stands out for presenting the highest relative percentage of forest coverage area (86.06 % in 2001 and 85.03 % in 2021), while the Madeira River basin records lower values 62.69 % in 2001 and 56.68 % in 2021, as depicted in Figure 4. It is also evident that only the Negro and Tapajós river basins experienced gains in forest cover, while the others underwent progressive losses.

Through the observation and interpretation of the six graphs (Figure 4) illustrating the behavior of forest formation in square kilometers, patterns and subtleties are delineated that bestow a more profound comprehension of the dynamics of these forest formations within this expansive region.

First, the Negro river subbasin stands out for demonstrating a smaller range of variation in forest cover loss compared to the other analyzed subbasins, with an approximate reduction of 1 % or $7,253\,km^2$. This consistency implies a strong commitment to preserving the region's forest wealth. Therefore, it is conceivable that specific interventions in environmental conservation could have played a fundamental role in maintaining this scenario. On the other hand, the subbasins of the Tapajós and Xingu rivers gain prominence, characterized by more pronounced oscillation indicators, which allude to an exacerbated trend of deforestation. In the Tapajós river subbasin, a notable 10 % reduction in forest area is evident, totaling $348,204\,km^2$, while in the Xingu river subbasin, a loss of 11 % was recorded, equivalent to $46,883\,km^2$. These fluctuations over the historical period reflect a more substantial human impact on forest cover in these regions. Agricultural expansion, intensive livestock farming, timber-related activities and mining can potentially play a catalytic role in this outcome.

Furthermore, the subbasins of the Solimões and Madeira rivers present oscillation patterns that are like those observed in the Amazon basin. However, it is important to highlight that the Madeira and Solimões subbasins found reductions of 10 % ($82,762\,km^2$) and 2 % ($39,961\,km^2$), respectively, in their forest formations. This behavior is, at a certain degree, in contrast, to the Amazon basin deforestation rate, where a cumulative loss of forest cover of 6 % was witnessed, totaling $265,162\,km^2$. Complementarity, relatively stable deforestation rates over time suggest a substantial impact of anthropogenic and economic influences on the region.

it should be noticed that, it becomes fundamental to emphasize the intrinsic link between the behavior of these subbasins and their undeniable territorial importance within the Amazon basin. This connection stems from the greater territorial representation of the subbasins of the Solimões and Madeira rivers in relation to their counterparts. Their extensive territorial coverage in the Amazon basin positions them as the most accurate reflections of the trends that characterize the region.

Preprints (www.preprints.org) | NOT PEER-REVIEWED | Posted: 9 October 2023 doi:10.20944/preprints202310.0383.v1

Finally, it is worth mentioning that the analysis of the graphs reveals common trends among the subbasins. Notable among them is a notable deceleration in deforestation between 2003 and 2013 and a more substantial reduction in forest loss becoming apparent in 2021.

A crucial aspect to analyze is the trend of decelerating deforestation over the years in all the mentioned subbasins, except for the period between 2020 and 2021, during which there was a significant increase in deforestation. This slowdown in deforestation implies the feasibility of controlling the expansion of an extensive agricultural frontier through an integrated array of measures, including surveillance, interventions in the soy and livestock production chains, credit access limitations, and other policy guidelines for planning and administrative management [25].

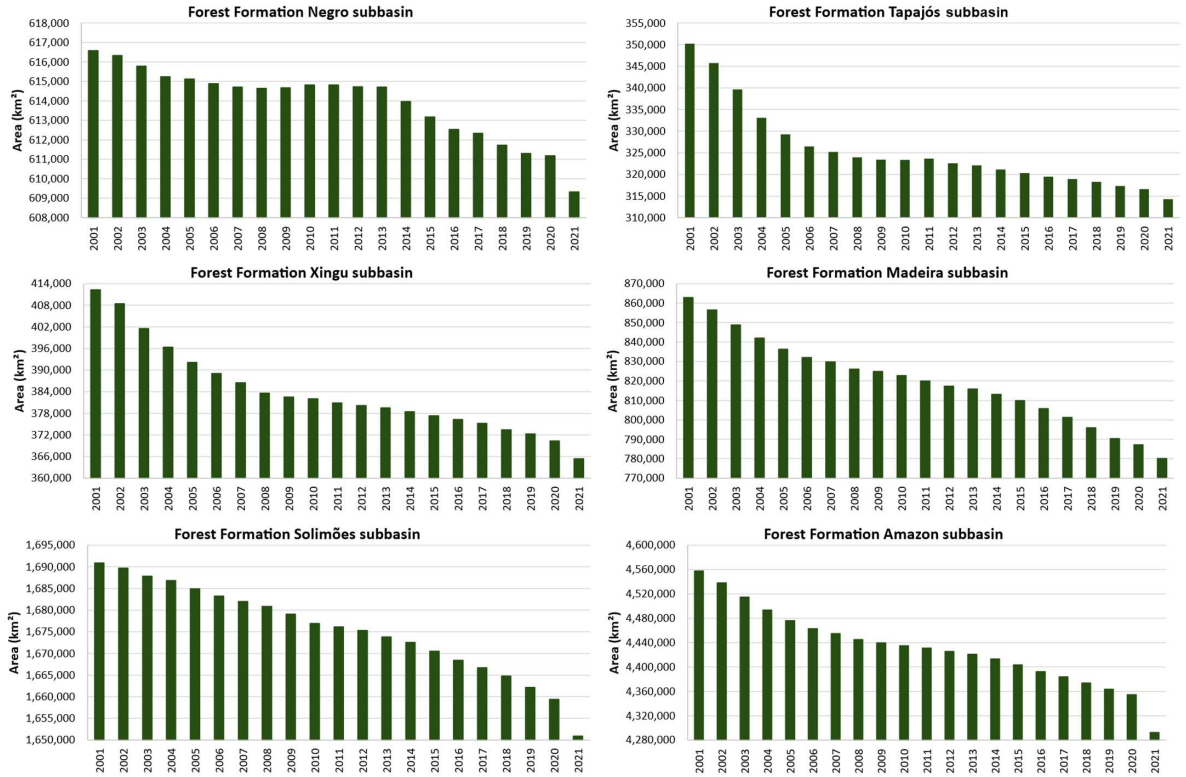

Figure 4. Subbasins dynamics of forest cover. Gains and losses for the main subbasins of the Amazon river basin along of 2001-2021 period.

3.2. Changes in LULC and transition rates in the Amazon basin

To obtain deeper insight into the specifics of the locations, amounts and types of changes in LULC, a plugin was used that allows the combination of different changes in LULC between two images from different years (2001 and 2021). The Semi-Automatic Classification Plugin (SCP) facilitates supervised classification of remote sensing images by providing tools for image download, prepossessing and post-processing.

The map in Figure 5 illustrates the main changes in LULC that occurred between 2001 and 2021. Among the most striking transitions, it is evident that the most significant changes in the Amazon basin are related to the expansion of Pasture areas (198, 193 km^2) and Agricultural areas (90, 784 km^2). Subsequently, the increase in Forest Formation (48, 445 km^2), Agriculture and Pasture Mosaic (46, 739 km^2) and Grassland (36, 1987 km^2) is remarkable.

However, when examining categories that reflect the preservation of the area, the Forest Formation gains prominence. Of the 4, 292, 565 km^2 of existing area in 2021, 97 % remained unchanged. On the other hand, only a minimum proportion of 1.23 % of the total area in 2021 transitions to the Forest Formation category. This situation plays a central role in explaining the sharp deforestation, which becomes more visible over the historical series of LULC.

Preprints (www.preprints.org) | NOT PEER-REVIEWED | Posted: 9 October 2023 doi:10.20944/preprints202310.0383.v1

When introducing this analysis, it is essential to highlight that, in the context of changes in LULC, some categories present remarkable levels of preservation. Among these categories, Fields (84 %) and Pastures (47 %) stand out as notable examples. These preservation patterns are intrinsically linked to the substantial transitions that occurred, contributing to a better understanding of the expansion of these categories over the historical series.

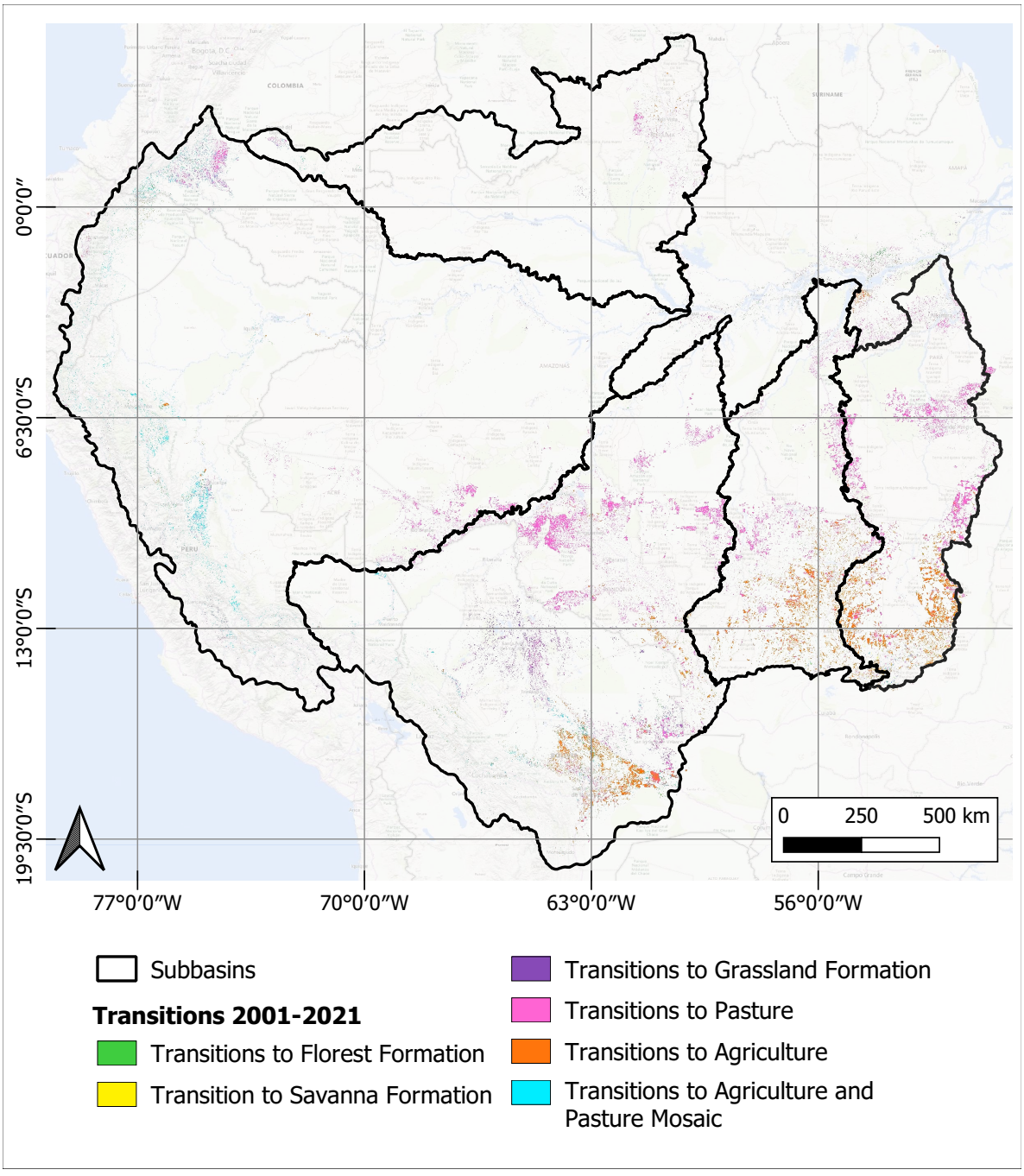

Figure 5. Transition map of the most expressive LULC classes in the Amazon basin.

3.3. Transition rates for subbasins

An analysis of transitions in LULC and occupation was carried out in the Amazon basin, focusing on the five main subbasins: Tapajós, Xingu, Madeira, Solimões and Negro, in order to obtain a deeper understanding of changing trends.

Preprints (www.preprints.org) | NOT PEER-REVIEWED | Posted: 9 October 2023 doi:10.20944/preprints202310.0383.v1

In all subbasins, there was a significant predominance in the conservation of forest formations. However, the Xingu and Negro rivers subbasins deserve special attention because they exert a deeper influence on the preservation of these formations, with rates of 71 % and 82 %, respectively, considering the total area of the subbasins. In the other subbasins, the proportions are 63 % for the Tapajós river, 74 % for the Solimões river and 55 % for the Madeira river.

Overall, the subbasins recorded limited occurrences of transitions. The Negro river subbasin recorded occurrences of 8 % conservation of Grassland and 2 % transformation of Forest Formations into Pastures, leaving 1 % for the other categories.

In the Tapajós river subbasin, a predominance of 22 % was observed in the preservation of Pastures, Agriculture and Grassland, while 6 % represent changes from Forest Formation to Pasture, 3% from Pasture to Agriculture and 2% from Forest Formation to Agriculture. The remaining proportions are of minor significance.

In the Solimões river subbasin, the transition of 7 % of Planted Forest to Forest Formation and 7 % of conservation of uses such as Pastures, Agriculture and Grassland is remarkable.

The Xingu river subbasin presents 8 % of transitions directed from forest formation to Pasture, 9 % for preservation of Pasture and Savanna Formation, 3 % in the transition from Pasture to Agriculture, in addition to other minor proportions.

Finally, in the Madeira river subbasin, 8 % of Planted Forests are transformed into Forest Formations, 13 % represent the preservation of Pastures and Grassland, 4 % of Forest Formations are lost to Pasture and 1 % to Agriculture.

The areas where the largest areas of forest recovery occur occur in Agriculture and Pasture areas ($8,817.0\,km^2$) in the Solimões river subbasin, located in the southern part of the Solimões river basin. Amazon.

The forest usually regenerates in abandoned pasture and cultivated areas when productivity declines. Consequently, fire is used in these areas for land clearing when the invasion of weeds and woody shrubs cannot be avoided [26].

The study of the characteristics of the secondary forest that grows in these abandoned pastures and cultivated areas shows that both the soil and the foliage of the young trees have less nitrogen than in the mature forest, due to the nitrogen loss that occurs in these burned areas used for deforestation. Only after decades of forest recovery does the nitrogen cycle rebalance, and this recovery time depends on the historical use of fire in these areas [27].Despite the numerous LULC transitions, it is important to highlight that success percentages still exhibit modest values. The areas undergoing forest regeneration, although increasing, encompass less than 2% of the total extent of each subbasin. This reality underscores the significant challenges surrounding ecological restoration and the recovery of forest ecosystems in previously deforested or degraded landscapes. In this context, it is crucial to intensify efforts to drive forest regeneration, seeking more effective methods of management, awareness, and conservation policies. Only through a coordinated and committed approach will it be possible to substantially increase the restored forest areas and, consequently, the environmental and socioeconomic benefits they provide.

3.4. Effects of Forest Coverage on the Water Balance at the subbasin Scale

Although remote sensing data require regional validation, they are considered sufficiently accurate to identify relative spatiotemporal variability at basin scale, especially for processes of interest such as P and ET. The time series generated for each subbasin are described in Figure 6. From this, greater amplitudes are observed in the interannual variations in the time series of the P, particularly notable in the subbasins of the Madeira, Tapajós and Xingu rivers, when compared to the Amazon basin. The analyzes revealed notable differences in the subbasins of the Xingu, Tapajós and Madeira rivers, when compared to other subbasins in the Amazon region. The mentioned subbasins have data with greater amplitude, which differs from the pattern observed in the data for the basin as a whole.

Preprints (www.preprints.org) | NOT PEER-REVIEWED | Posted: 9 October 2023 doi:10.20944/preprints202310.0383.v1

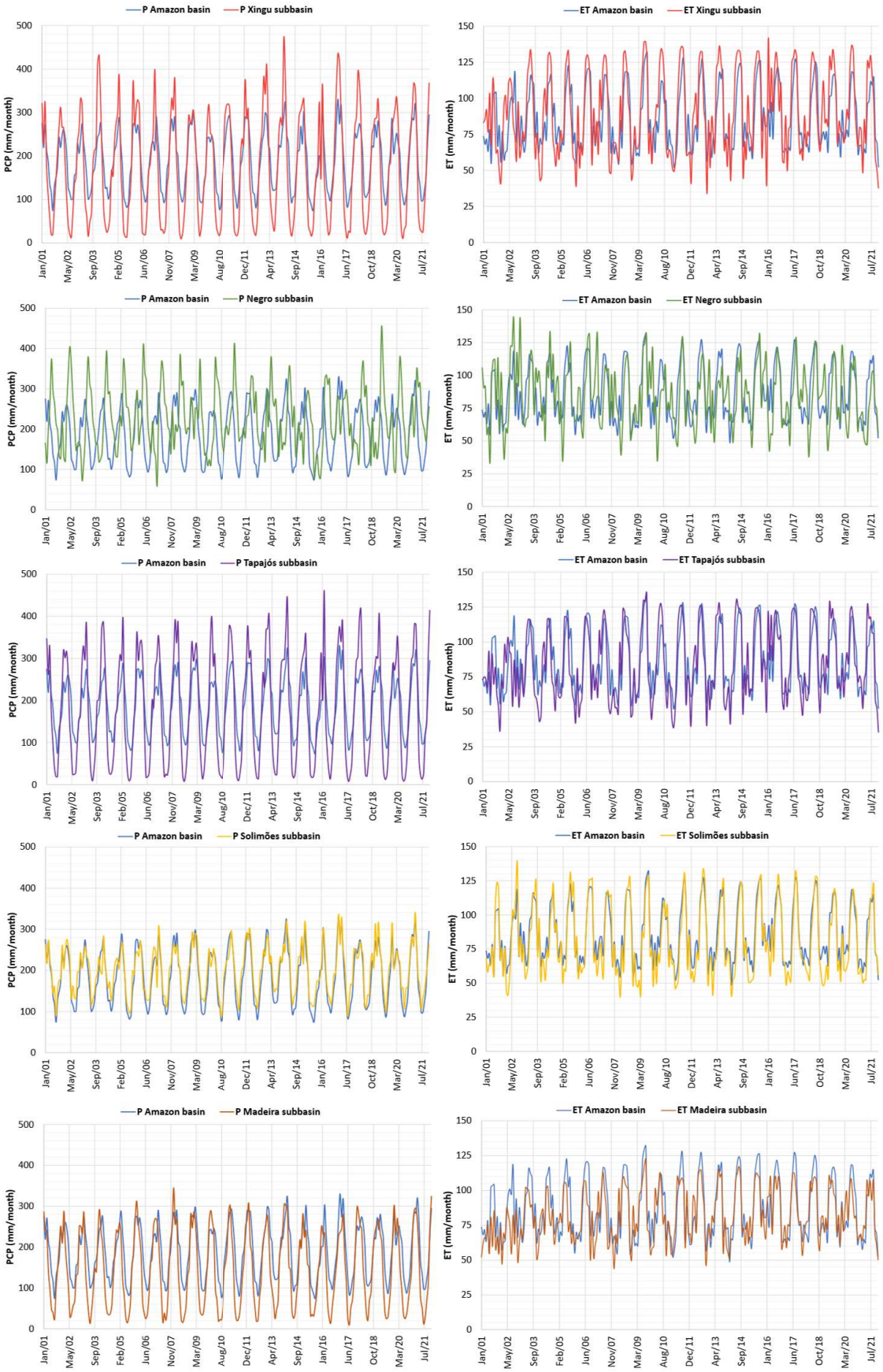

Figure 6. Historical time series of P and ET for the studied subbasins compared to the Amazon basin.

Preprints (www.preprints.org) | NOT PEER-REVIEWED | Posted: 9 October 2023 doi:10.20944/preprints202310.0383.v1

The cohesion identified between the Xingu, Tapajós and Madeira subbasins, which supports the extreme variations recorded, can be attributed mainly to more intense changes in LULC due to anthropogenic activities, notably in agriculture and pasture. The proliferation of these human practices may have triggered marked transformations in local ecosystems, resulting in remarkable changes in hydrological and environmental patterns.

In the other hand, the Negro river subbasin presents a unique characteristic in its data. Its patterns do not harmonize with the prevailing scenario observed in the Amazon Basin.

The uniqueness observed in the Negro river subbasin can be explained by its distinct composition in terms oF LULC. In this region, it is notable the predominance of vast areas of natural vegetation and a lower incidence of anthropogenic interventions aimed at agriculture and pasture. This particular environmental configuration can influence hydrological dynamics, biodiversity and flow patterns in the subbasin, contributing to the discrepancies shown in the data. This peculiarity further emphasizes the need to consider the specific contexts of each subbasin when formulating sustainable management and conservation policies and practices. It is essential to highlight that this analysis coincides with the deceleration of the deforestation rate for the period shown in Figure 4.

The most enlightening results are evident in Figure 7, where the better-preserved subbasins, such as the Negro River subbasin, exhibit higher accumulated P and ET volumes over the years. On the other hand, the less-preserved subbasins with significant LULC changes, such as the Madeira River subbasin, show lower accumulated P and ET volumes over the years. The observed data reveal a concerning imbalance between P-ET in three key years, 2010, 2015, and 2020, due to severe drought. Over the years, there has been a significant shortage of water resources, with evapotranspiration exceeding precipitation, leading to a drastic reduction in available water resources. The lack of rainfall during these periods has serious consequences for some regions, affecting not only water supply but also agriculture, wildlife, and the quality of life of local communities. Considering this data, it is essential to adopt sustainable water management measures and plan adaptation strategies to address the growing threat of climate change.

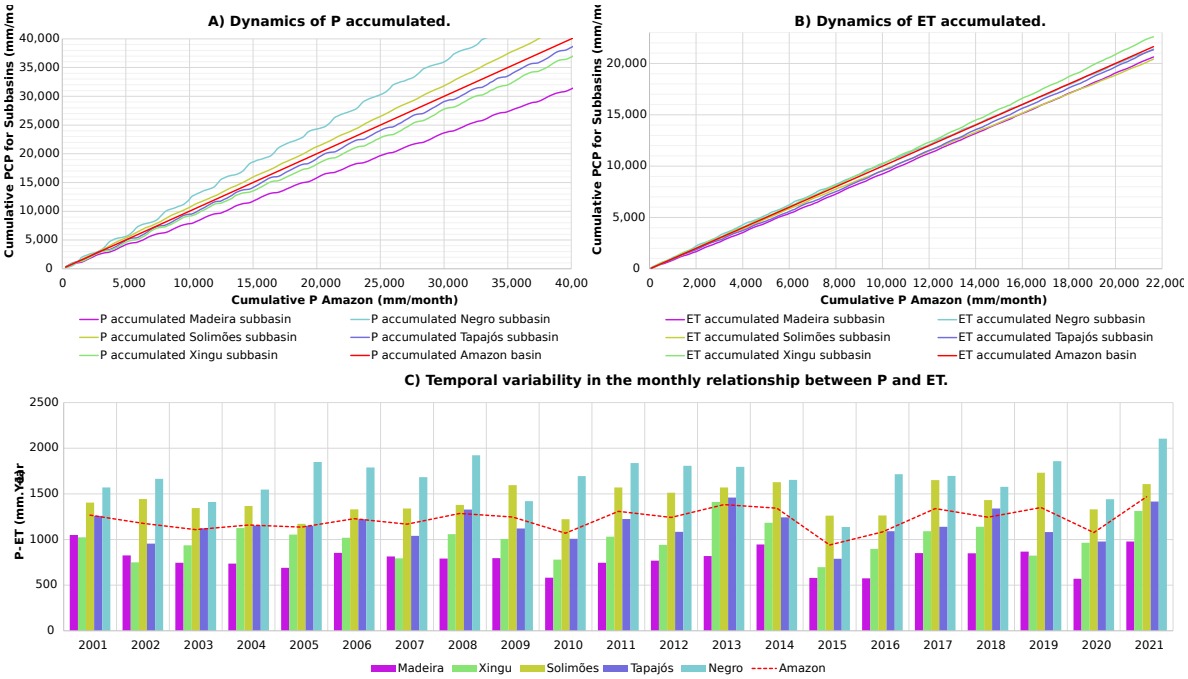

Figure 7. Dynamics of P and ET accumulated over the years (2001-2021) in the Amazon basin and in its main subbasins (Negro, Solimões, Madeira, Tapajós and Xingu)

When comparing the average P and ET in the Amazon basin (Figure 8), the values increased between the years 2013 to 2021 (ET: 1042.22 mm ; P: 2286.10 mm) compared to the period from 2001

Preprints (www.preprints.org) | NOT PEER-REVIEWED | Posted: 9 October 2023 doi:10.20944/preprints202310.0383.v1

to 2006 (ET: 1018.17 mm; P: 2213.30 mm), resulting at an increase of 2.36 % and 3.26 %, respectively. Considering the annual average from 2001 to 2021 (ET: 1, 030.20 %; P: 2, 249.69 %), it is evident that the averages for the periods from 2012 to 2021 exceed the overall historical average. This result suggests that the second half of the time series has a greater influence on the data, indicating possible significant changes in hydrological processes over time.

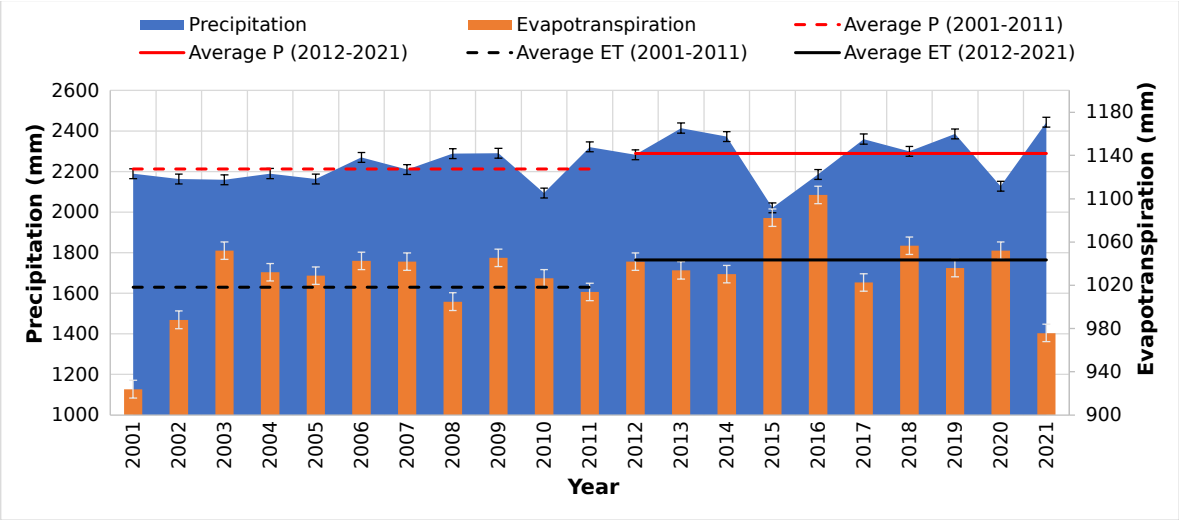

Figure 8. Comparing the average P and ET over Amazon basin in 2001-2011 and 2012-2021 time periods.

When the relationship between ET and P (ET/P, percentage) is analyzed separately for eash basin, as shown in Table 2, we observe that the most preserved area (minimum deforestation) corresponding to the subbasin Negro basin has the lowest proportion, where ET represents 38% of the total P, while the Madeira subbasin has the highest rate, with ET representing 56% of the total P volume in the basin. The average ET (1,030.20 mm/year) corresponds to 46% of the P (2,249.69 mm/year) for the entire Amazon basin in the period from 2001 to 2021. The biggest difference between P and ET in the entire Amazon basin occurred in 2021, indicating the driest year of the study period (2001-2021).

Table 2. Annual average of the ET/P ratio for each subbasin from 2001 to 2021.

Subbasins	P annual average(mm.year-1)	ET annual average (mm.year-1)	Dif. (ET/P (%))
Negro	2,693.8	1,019.7	38%
Solimões	2,408.3	972.9	40%
Tapajós	2,167.9	1,015.7	47%
Xingu	2,077.9	1,076.5	52%
Madeira	1,763.6	982,0	56%
Amazon	2,249.7	1,030.2	46%

In addition, 2021 was the wettest year in the historical series, with the lowest recorded ET values. At the subbasin scale, the ET (P percentage) is more significant in the southern region of the Amazon basin (Madeira: 56%; Xingu: 50%; Tapajós: 47%), which can be considered the subbasin with lower P values. On the other hand, the increase in ET north of the Negro subbasin has a less pronounced influence on the water balance, with 38%.

Thus, it is expected that, in the long term, if the storage capacity of the basin decreases, the amount of water released in the subbasin of the Negro will be considerably influenced by changes in the precipitation pattern that occur in this region. These changes in the precipitation regime will have a specific impact on the amount of water available for the runoff of the Negro compared to other subbasins. The increase in the area of preserved Amazon rainforest due to lower deforestation rates

Preprints (www.preprints.org) | NOT PEER-REVIEWED | Posted: 9 October 2023 doi:10.20944/preprints202310.0383.v1

corroborates with the increase in average P and ET rates. It is evident that, based on these results, there is a significant interdependence in forest preservation and the intensification of P and ET rates in the main subbasins under scenarios of global climate change and increased frequency of extreme weather events.

These developments point to the importance of regular monitoring of hydrological variables through remote sensing platforms and in situ networks, to provide an adequate framework for analysis and development of more effective forest preservation and management policies. These practices will benefit the guarantee of sustainable water supply in terms of quantity and quality, energy production and food supply, together with the improvement of ecosystem services and economic and social aspects at the basin scale.

In the adopted period, the years 2010, 2015 and 2020 had lower mean P values for the entire basin. On the other hand, the years 2013, 2017, 2019 and 2021 showed a high volume of rainfall. It can be observed that the subbasins of the South region (Madeira, Xingu, Tapajós) have the lowest rainfall volumes, mainly in the months of May, June, July and August, as shown in Figure 9. It is also noticed that the highest P values are concentrated in the northernmost region, from April to September, represented by the colors green and blue, which does not occur in the rest of the basin, suggesting that the Negro subbasin has a greater amplitude in P values.

The years 2015 and 2016 exhibited notably high average evapotranspiration (ET) across the entire Amazon basin. In contrast, the years 2001, 2002, 2008, 2011, 2017, 2019, and 2021 recorded ET values below the anticipated average. As depicted in Figure 10, subbasins in the southern region (Madeira, Tapajós, and Xingu) displayed lower ET values from November to February, but higher ET values from March to October. Conversely, for more northern subbasins like Negro, the pattern was reversed. Notably, the Solimões subbasin exhibited greater fluctuations in ET values.

Comparing the disparity between average precipitation and ET over time, distinct water deficits were evident during the periods of 2011-2012 and 2015-2017. The Solimões subbasin mirrored the average P and ET trends of the entire Amazon, while the southern subbasins (Madeira, Tapajós, and Xingu) demonstrated larger P and ET variations with more pronounced amplitudes compared to the overall Amazon basin average. Moreover, there was an approximate one-month lag between peak rainfall in the Negro subbasin and the average P of the entire Amazon basin, linked to a P regime [13]. Strong seasonality and interannual variability were evident in both series.

Preprints (www.preprints.org) | NOT PEER-REVIEWED | Posted: 9 October 2023 doi:10.20944/preprints202310.0383.v1

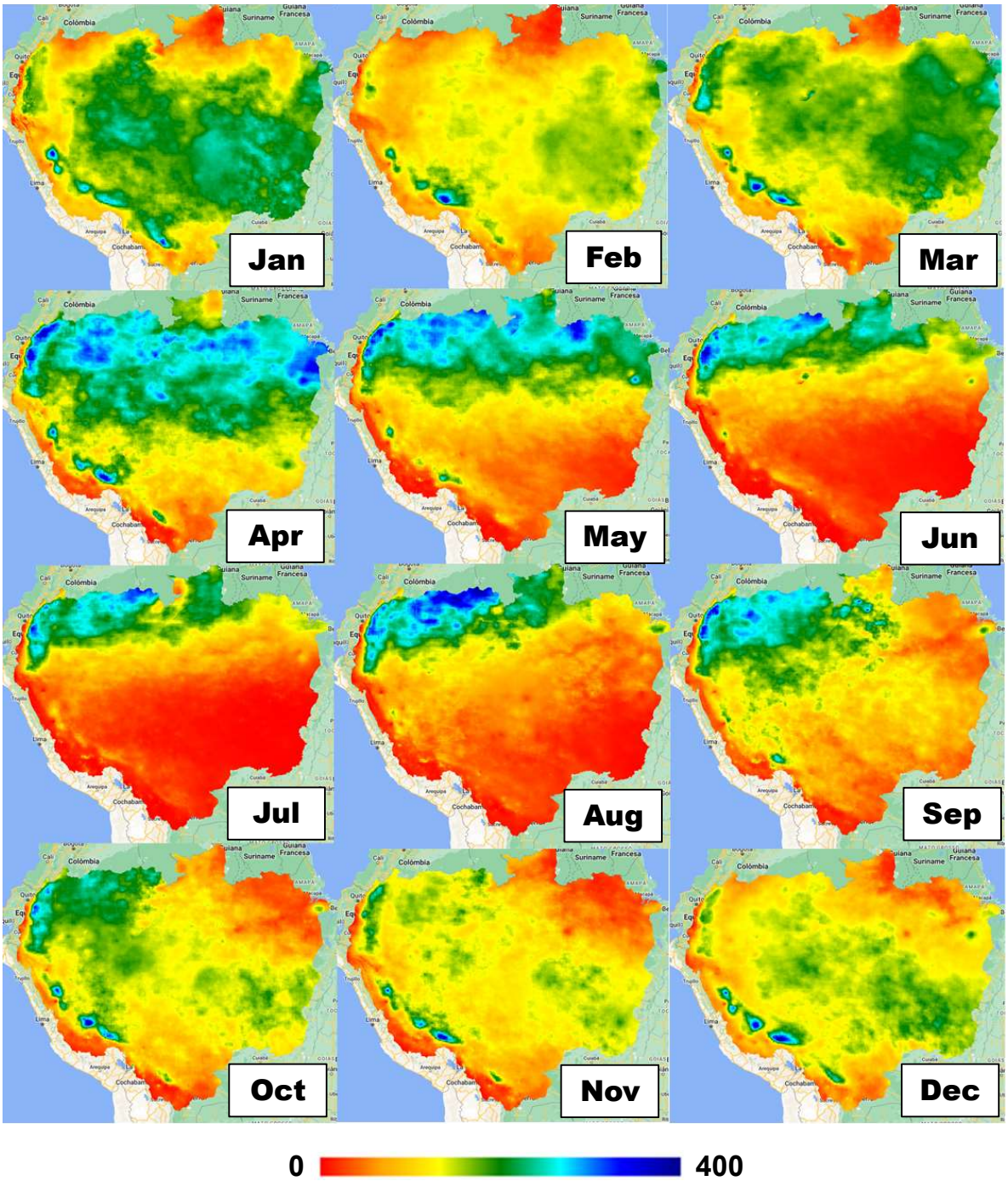

Figure 9. Spatial distribution of average monthly precipitation based on CHIRPS for the Amazon basin.

Preprints (www.preprints.org) | NOT PEER-REVIEWED | Posted: 9 October 2023 doi:10.20944/preprints202310.0383.v1

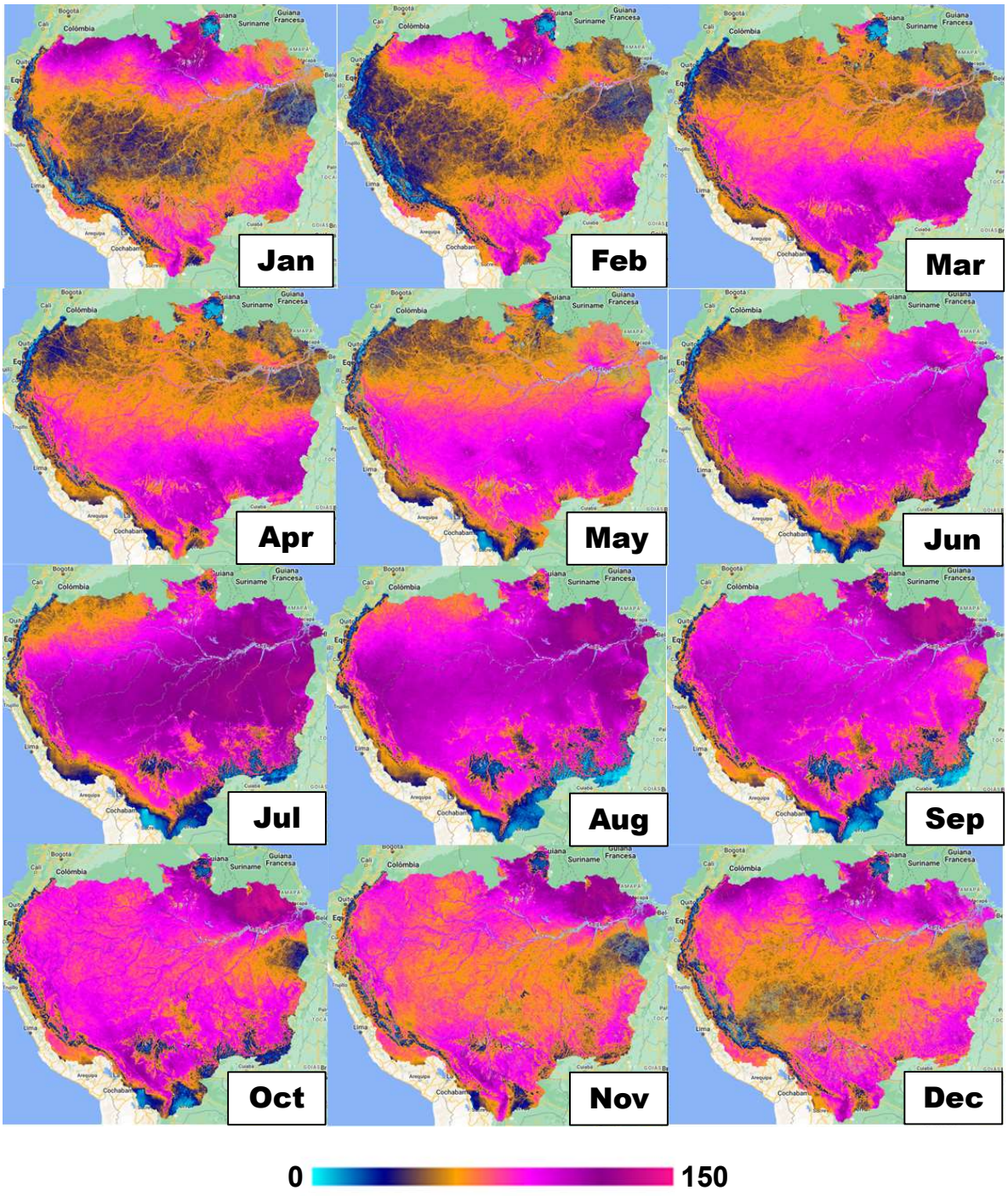

Figure 10. Mean monthly spatial distribution of spatial evapotranspiration based on MODIS-MOD16A2 for the Amazon basin.

3.5. The influence of highways on LULC in the Brazilian Amazon

The Amazon Basin, one of the most biodiverse and ecologically significant regions in the world, has been profoundly affected by the influence of highways on LULC. These transportation routes, many of which were constructed to promote economic development and regional integration, have played a pivotal role in reshaping the Amazonian landscape. By connecting remote areas to urban centers and markets, highways have facilitated access to natural resources, deforestation, agricultural expansion, and colonization. To illustrate this intricate process of change, Figure 11 visually depicts how road

Preprints (www.preprints.org) | NOT PEER-REVIEWED | Posted: 9 October 2023 doi:10.20944/preprints202310.0383.v1

networks have penetrated and shaped the Amazon Basin over time, highlighting the interplay between transportation corridors and the transformation of the surrounding environment.

After the construction of highways in the Amazon basin, significant changes occurred in the scenario of urban settlements and transportation. Before this infrastructure, urban settlements were restricted to the riverbanks, and transportation was predominantly carried out through waterways [28].

The opening of roads in the second half of the 20th century triggered a series of transformations in the region. It stimulated colonization and the development of agricultural frontiers into the interior of the Amazon basin. However, unfortunately, it also intensified deforestation and had impacts on land cover. Several reasons drove the construction of these roads in the Amazon. Regional integration, stimulation of economic development with access to the global market, and geopolitical security concerning the borders were some of the main objectives [29].

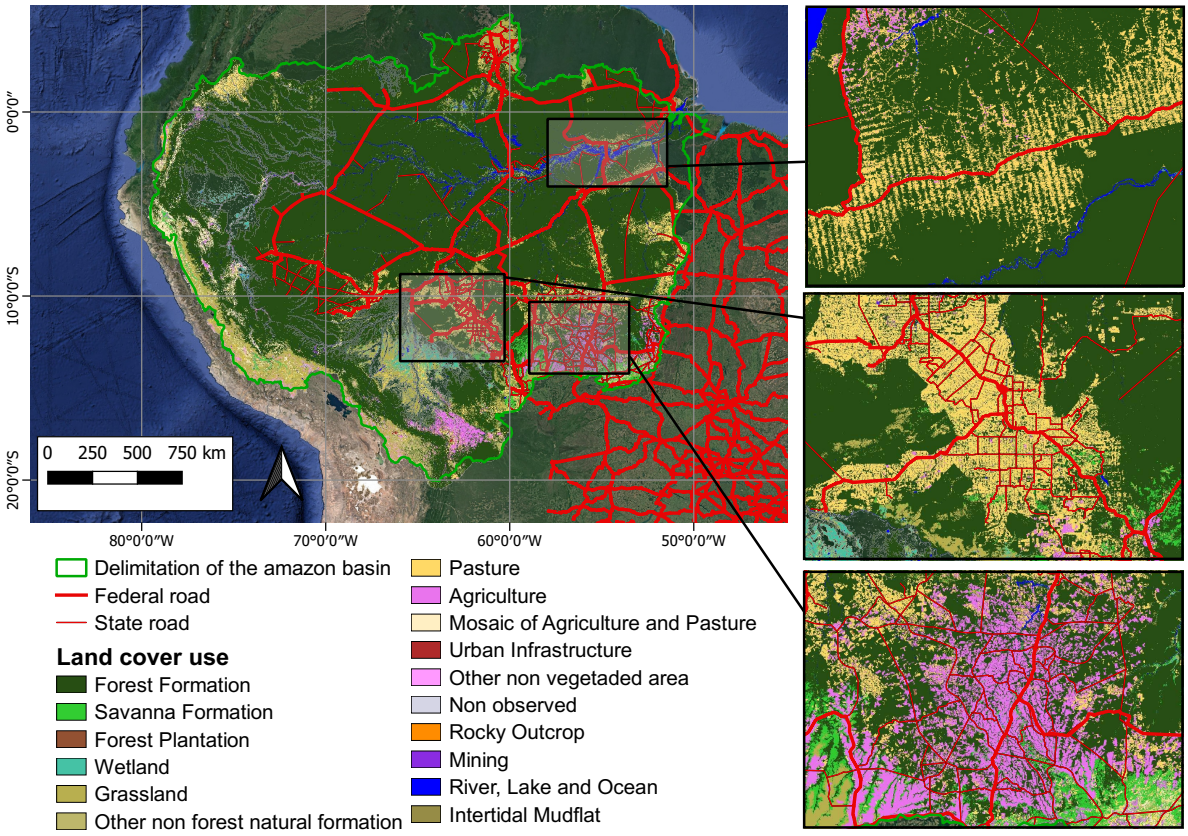

Figure 11. Roads over the Brazilian Amazon jointly with the land use and land cover in the Amazon region.

The first highway built in the region, the Belém-Brasília, completed in 1964, had a direct impact on the environment. It resulted in the uncontrolled expansion of pasture areas for cattle ranches in the southern region of the state of Pará. Additionally, colonization projects in the Brazilian Amazon were also significant sources of deforestation, especially along the highways, where a characteristic pattern known as the "fishbone" pattern was created [30,31].

This pattern consists of perpendicular crossings approximately 10 km apart in both directions of the highways, forming an arrangement that aims to extend land tenure and ensure livelihoods for families [32].

Currently, the regions with the highest density of highways in the Amazon basin are those that underwent the most significant changes in LULC. This dense road network can be observed in Figure 11 in the pastureland region and also in the cultivated land area in the southeast of the Amazon basin. The representation of the "fishbone" pattern is evident in the first enlargement of the image. The

Preprints (www.preprints.org) | NOT PEER-REVIEWED | Posted: 9 October 2023 doi:10.20944/preprints202310.0383.v1

increased demand in the international market for soybeans further drove investments in infrastructure, leading to the construction and maintenance of roads for the transportation of production [33].

4. Discussion

In this section, initially, we present some world well known research works [28,34–37]. After a more detailed presentation of each of such works, we then present the contributions of this paper in comparison with the previous cited methodological approaches.

To initiate this investigation, we will address the relationship between the El Niño and La Niña years identified by the National Oceanic and Atmospheric Administration (NOAA) and the water balance in the Amazon basin as a whole.

El Niño is a large-scale climatic phenomenon that significantly impacts weather patterns in various parts of the world, including South America. During El Niño years, the Equatorial Pacific Ocean is warmer than the historical average, triggering global effects on atmospheric circulation patterns, moisture transport, temperature, and precipitation. To be classified as an El Niño event, temperature anomalies must exceed 0.5°C for at least five consecutive three-month periods. La Niña, on the other hand, is also a large-scale climatic phenomenon with significant impacts on global climate patterns. During La Niña years, the Equatorial Pacific Ocean has temperatures below the historical average, resulting in global effects on atmospheric circulation patterns, moisture transport, temperature, and precipitation. To be classified as a La Niña event, temperature anomalies must be less than -0.5°C for at least five consecutive three-month periods [41].

The analysis of El Niño and La Niña years and their impacts on the mentioned variables seeks a deeper understanding of how these phenomena influence the environment and weather conditions in different regions of the country. This analysis plays a crucial role in the development of strategies for adapting to and mitigating extreme weather events, as well as in the sustainable planning of LULC and water resources.

Examining the historical series covering the years from 2001 to 2021, according to the records of the National Oceanic and Atmospheric Administration (NOAA), we identified that the periods of 2002-2003, 2004-2005, 2006-2007, 2009-2010, and 2015-2016 were El Niño years, with the periods of 2009-2010 and 2015-2016 being the most critical.

Analyzing the historical series obtained for the Amazon basin, it is observed that these mentioned years coincide with low precipitation levels and higher evapotranspiration values, especially in the years 2010 and 2015. Therefore, when analyzing the water balance of the historical series, it becomes evident that these two aforementioned years had lower annual values, highlighting the influence of the phenomenon on the basin.

Furthermore, considering the La Niña years identified by NOAA within the historical series addressed in this study, notable periods include 2005-2006, 2007-2008, 2008-2009, 2010-2011, 2011-2012, 2016-2017, 2017-2018, and 2020-2021. In this study, it is observed that this phenomenon exerted greater influence in the years 2008, 2011, 2017, and 2021, during which above-average precipitation and below-average evapotranspiration were recorded.

Throughout the analysis of the historical series, it becomes evident that both El Niño and La Niña phenomena were less noticeable at the beginning of the period under consideration. However, as time progressed, these phenomena became more frequent and intense. This trend may be intrinsically related to various variables, including deforestation and significant changes in LULC.

Deforestation, which results in the removal of extensive areas of natural vegetation, can significantly alter climate patterns in affected regions. The removal of trees and vegetation can influence evapotranspiration, heat absorption, and local atmospheric circulation, which, in turn, can affect the occurrence and intensity of climatic phenomena such as El Niño and La Niña.

Furthermore, LULC changes, such as the conversion of forests into urban, agricultural, or livestock areas, can alter surface patterns, including moisture retention and release capacity. These changes

Preprints (www.preprints.org) | NOT PEER-REVIEWED | Posted: 9 October 2023 doi:10.20944/preprints202310.0383.v1

can have a considerable impact on local and regional climate conditions, making climate variations associated with El Niño and La Niña more perceptible and impactful.

Therefore, the intensification and increasing perceptibility of El Niño and La Niña phenomena throughout the historical series may be directly related to environmental transformations, such as deforestation and LULC changes, which have modified climatic characteristics on a regional and global scale. These observations underscore the importance of sustainable environmental management and proper LULC planning as crucial measures for addressing the growing climate changes and their impacts.

As this analysis unfolded, it became clear that the El Niño and La Niña phenomena are playing increasingly prominent roles in our climate scenario, with their influences becoming more pronounced over time, possibly due to factors such as deforestation and LULC changes. These conclusions underscore the urgent need to direct our efforts towards deeper and more specific investigations.

The next steps in our scientific journey should be closely related to hydrological studies, specifically aimed at understanding rainfall-runoff behavior in regions affected by these climatic phenomena. Understanding the hydrological cycle, including how rainfall transforms into runoff and how rivers respond to these changes, is crucial for effective water resource management and for mitigating the impacts of extreme events.

Furthermore, integrating hydrological data with climate and LULC models can open up new perspectives in predicting and managing climate events. This interdisciplinary approach empowers us to take proactive measures for environmental conservation, sustainable urban and agricultural planning, and ensuring water security in the face of ever-evolving climate challenges.

5. Conclusions

In conclusion, this study provides a profound insight into the intricate interactions among deforestation, forest conservation, and the water cycle within the Amazon basin. The findings underscore the urgency of preserving forests as a fundamental component in maintaining the characteristic hydrologyical features of the region. Understanding the connections between the patterns of P and ET, influenced by sociopolitical factors, yields valuable insights for informed decision-making regarding the sustainable management of this vital ecosystem for the planet.

The notable changes in LULC and vegetation cover within the Amazon subbasins from 2001 to 2021 emphasize the importance of conservation practices to mitigate losses. Notably, a reduction in forest cover is evident in most sub-basins, except for the Negro river subbasin, which exhibits the highest percentage of undisturbed forest (1.2% deforestation). This observation can be attributed to minimal interventions in terms of LULC. Consequently, in other subbasins, the greatest loss of forest cover occurred in forested areas, while regions of pasture and agriculture experienced significant expansion.

The subbasins undergoing the most profound transformations in LULC also exhibit wide variations in P and ET data. Notably, regions located to the south, such as the Madeira, Tapajós, and Xingu river subbasins, recorded pronounced fluctuations in P and ET patterns. This translates to more severe droughts and periods of intensified rainfall, thereby highlighting the impact of LULC changes on local climatic conditions. This direct relationship between land transformations and climatic extremes reinforces the need for integrated approaches that consider both forest conservation and hydrological equillibrium to ensure the resilience of these evolving regions.

The striking decrease in Forest Formation also underscores the need to investigate the underlying causes of this trend and comprehend its implications for the overall sustainability of the Amazon ecosystem.

Preprints (www.preprints.org) | NOT PEER-REVIEWED | Posted: 9 October 2023 doi:10.20944/preprints202310.0383.v1

The construction of roads and highways within the Amazon basin has had a profound impact on vegetation cover, resulting in deforestation and in the expansion of agricultural areas. Consequently, the distinctive "fishbone" pattern created along highways due to colonization projects illustrates how the dense road network is associated with significant LULC changes, particularly in pasture and cultivation areas, driven by global demand for soy, for, for example, and food production in general.

Acknowledgments: The authors would like to acknowledge the financial support provided by the Brazilian National Council for Scientific and Technological Development (CNPq), Science Without Borders Program - CsF, Coordination for the Improvement of Higher Education Personnel (CAPES) and Research Support Foundation of the State of Minas Gerais (FAPEMIG), for conducting this research work. We also would like to express our special thanks to the Vadose Zone Research Group (VZRG) at Texas A&M University, the Department of Sanitation and Environmental Engineering (ESA) and Postgraduate the Civil Engineering Program (PEC) at Federal University of Juiz de Fora-UFJF, Juiz de Fora-MG, Brazil and the Civil Engineering Program - Alberto Luiz Coimbra Institute of Postgraduate and Engineering Research - COPPE/PEC/UFRJ for the cooperation with this study. We are also grateful to the MAPBIOMAS, and to the, GEE [39,40] for making available hydrological datasets for this research work.

Conflicts of Interest: The authors declare that there is no conflict of interest and the funders played an important role in the design of the study; in data collection, analysis and interpretation.

Sample Availability: Samples of the compounds ... are available from the authors.

Abbreviations

Abbreviations

The following abbreviations are used in this manuscript:

UFJF	Federal University of Juiz de Fora
UFRJ	Federal University of Rio de Janeiro
ET	Evapotranspiration
P	Precipitation
LULC	Land Use and Land Cover
GEE	Google Earth Engine
CHIRPS	Climate Hazards Group InfraRed Precipitation with Station data
MODIS	Moderate Resolution Imaging Spectroradiometer
GEE	Google Earth Engine

Appendix A. Algorithms used in temporal distribution - Evapotranspiration and Precipitation

The algorithms used on the GEE platform to obtain the temporal distribution of P and ET will be presented here-in.

Preprints (www.preprints.org) | NOT PEER-REVIEWED | Posted: 9 October 2023 doi:10.20944/preprints202310.0383.v1

Algorithm A1 Time series precipitation analysis - GEE

```
var area = ee.FeatureCollection('.../LimiteBacia');
var empty = ee.Image().byte();
var outline = empty.paint({featureCollection: area, color: 1, width: 2});
Map.addLayer(outline, {palette: '#000000'}, 'Amazon basin', 1);
Map.centerObject(area, 7);

var starting_year = 2001;
var final_year    = 2021;
var month    = ee.List.sequence(1,12);
var interval = ee.List.sequence(starting_year,final_year);
var start    = ee.Date.fromYMD(starting_year,1,1);
var end      = ee.Date.fromYMD(final_year,12,31);

var CHIRPS = ee.ImageCollection("UCSB-CHG/CHIRPS/DAILY").select('precipitation')
.filterDate(start,end).filterBounds(area);

var p_monthly = ee.ImageCollection.fromImages(
  interval.map(function(year){
    return month.map(function(month){
      var p_month = CHIRPS.filter(ee.Filter.calendarRange(year,year,'year'))
                          .filter(ee.Filter.calendarRange(month,month,'month')).sum().clip(area);

      return p_month.set('year',year).set('month',month).set('date',ee.Date.fromYMD(year,month,1))
      .set('system:time_start',ee.Date.fromYMD(year,month,1));});}).flatten());

var chartp_monthly = ui.Chart.image.series(p_monthly, area , ee.Reducer.mean(),2500,
    'system:time_start')
                    .setOptions({title: 'Accumulated monthly precipitation of the Amazon basin',
                      vAxis: {title: 'P (mm/month)'}});
  print(chartp_monthly);
```

Algorithm A2 Time series evapotranspiration analysis - GEE

```
var area = ee.FeatureCollection('.../LimiteBacia');
var empty = ee.Image().byte();
var outline = empty.paint({featureCollection: area, color: 1, width: 2});
Map.addLayer(outline, {palette: '#000000'}, 'Bacia Hidrográfica do Rio Amazonas', 1);
Map.centerObject(area, 7);

var starting_year = 2001;
var final_year = 2021;
var month = ee.List.sequence(1, 12);
var interval = ee.List.sequence(starting_year, final_year);
var start = ee.Date.fromYMD(starting_year, 1, 1);
var end = ee.Date.fromYMD(final_year, 12, 31);

var MODIS = ee.ImageCollection("MODIS/006/MOD16A2").select('ET').filterDate(start,
    end).filterBounds(area);

var et_monthly = ee.ImageCollection.fromImages(interval.map(function (year){return
    month.map(function (month) {var et_month = MODIS.filter(ee.Filter.calendarRange(year, year,
    'year')).filter(ee.Filter.calendarRange(month, month, 'month')).sum().clip(area).multiply(0.1);

return et_month.set('year', year).set('month', month).set('date', ee.Date.fromYMD(year, month, 1))
        .set('system:time_start', ee.Date.fromYMD(year, month, 1));});}).flatten()
);

var chartet_monthly = ui.Chart.image.series(et_monthly, area, ee.Reducer.mean(), 2500,
    'system:time_start')
  .setOptions({title: 'Accumulated monthly evapotranspiration of the Amazon basin',vAxis: { title:
    'ET (mm/month)'}});
print(chartet_monthly);
```

Appendix B. Algorithms used in spatial distribution - Evapotranspiration and Precipitation

The algorithms used on the GEE platform to obtain the spatial distribution of P and ET will be presented here-in.

Preprints (www.preprints.org) | NOT PEER-REVIEWED | Posted: 9 October 2023 doi:10.20944/preprints202310.0383.v1

Algorithm A3 Monthly precipitation analysis - GEE

```
var area = ee.FeatureCollection('.../LimiteBacia');
var ano_inicial = 2001;
var ano_final = 2021;
var month = 1; // Insert the desired month number here

var intervalo = ee.List.sequence(ano_inicial, ano_final);
var CHIRPS =
  ee.ImageCollection("UCSB-CHG/CHIRPS/DAILY").select('precipitation').filterDate(ano_inicial +
  '-01-01', ano_final + '-12-31').filterBounds(area);

var calcularPMensal = function(year, month) {
  var start = ee.Date.fromYMD(year, month, 1);
  var end = start.advance(1, 'month');
  var P_month = CHIRPS.filterDate(start, end).sum().clip(area);
  return P_month.set('year', year).set('month', month).set('date', start).set('system:time_start',
    start.millis());
};

var P_mensal = ee.ImageCollection.fromImages(
  intervalo.map(function(ano) {
    return ee.List.sequence(month, month).map(function(month) {
      return calcularPMensal(ano, month);
    });
  }).flatten()
);

var P_month = P_mensal.filter(ee.Filter.calendarRange(month, month, 'month'));
var P_month_mean = P_month.mean();
var month_stats = P_month_mean.reduceRegion({reducer: ee.Reducer.minMax(), geometry: area, scale:
  2500, maxPixels: 1e13});
var minP_month = month_stats.getNumber('precipitation_min');
var maxP_month = month_stats.getNumber('precipitation_max');
var paletteP_month = ['red','orange','yellow','green','cyan','blue','darkblue'];
var normalizedValues_month = P_month_mean.select('precipitation').unitScale(minP_month, maxP_month);
var P_month_vis = normalizedValues_month.visualize({ min: 0, max: 1, palette: paletteP_month });

var label = 'Média de Precipitação (Mês ' + month + ')';
Map.addLayer(P_month_vis, {}, label);
```

Algorithm A4 Monthly evapotranspiration analysis - GEE

```
var area = ee.FeatureCollection('.../LimiteBacia');
var ano_inicial = 2001;
var ano_final = 2021;
var month = 1; // Insert the desired month number here

var intervalo = ee.List.sequence(ano_inicial, ano_final);
var MODIS = ee.ImageCollection("MODIS/006/MOD16A2").select('ET').filterDate(ano_inicial + '-01-01',
  ano_final + '-12-31').filterBounds(area);

var calcularETMensal = function(year, month) {
  var start = ee.Date.fromYMD(year, month, 1);
  var end = start.advance(1, 'month');
  var et_month = MODIS.filterDate(start, end).sum().clip(area).multiply(0.1);
  return et_month.set('year', year).set('month', month).set('date', start).set('system:time_start',
    start.millis());
};

var et_mensal = ee.ImageCollection.fromImages(intervalo.map(function(ano) {
  return ee.List.sequence(month, month).map(function(month) {
    return calcularETMensal(ano, month);
  });
}).flatten());

var et_month = et_mensal.filter(ee.Filter.calendarRange(month, month, 'month'));
var et_month_mean = et_month.mean();

var month_stats = et_month_mean.reduceRegion({reducer: ee.Reducer.minMax(), geometry: area, scale:
  2500, maxPixels: 1e13});
var minET_month = month_stats.getNumber('ET_min');
var maxET_month = month_stats.getNumber('ET_max');

var paletteET_month = ['cyan', 'darkblue', 'orange', 'Magenta', 'DarkMagenta', 'DeepPink'];
var ET_month_vis = et_month_mean.select('ET').unitScale(minET_month, maxET_month).visualize({ min: 0,
  max: 1, palette: paletteET_month });

var label = 'Mean Evapotranspiration (Month ' + month + ')';
Map.addLayer(ET_month_vis, {}, label);
```

Preprints (www.preprints.org) | NOT PEER-REVIEWED | Posted: 9 October 2023 doi:10.20944/preprints202310.0383.v1

Appendix C. Repository

www.github.com/eduardatf/FilgueirasMDPI2023

References

1. Barthem, R.B., P. Charvet-Almeida, L.F.A. Montag and A.E. Lanna. Amazon Basin, GIWA Regional assessment 40b. *Sweden, University of Kalmar/UNEP* **2004**. 60p.
2. Malhi, Y., Wood, D., Baker, T.R., Wright, J., Phillips, O.L., Cochrane, T., Meir, P., Chave, J., Almeida, S., Arroyo, L. and others. The regional variation of aboveground live biomass in old-growth Amazonian forests. *Global Change Biology* **2006** vol. 12, n.7, 1107–1138.
3. Saatchi, S.S., Houghton, R.A., Dos Santos Alvala, R.C., Soares, J.V., Yu, Y. Distribution of aboveground live biomass in the Amazon basin. *Global Change Biology* **2007** vol. 13, n.4, 816–837.
4. Davidson, E.A., de Araujo, A.C., Artaxo, P., Balch, J.K., Brown, I.F., Bustamante, M.M.C., Coe, M.T., DeFries, R.S., Keller, M., Longo, M. and others. The Amazon basin in transition. *Nature* bf 2012. vol. 481, n.7381, 321–328.
5. Asner, G.P., Knapp, D.E., Broadbent, E.N., Oliveira, P.J.C., Keller, M., Silva, J.N. Selective logging in the Brazilian Amazon. *Science* **2005** vol. 310, n.5747, 480–482.
6. Macedo, M.N., DeFries, R.S., Morton, D.C., Stickler, C.M., Galford, G.L., Shimabukuro, Y.E. Decoupling of deforestation and soy production in the southern Amazon during the late 2000s. *Proceedings of the National Academy of Sciences* **2012** vol. 109, n.4, 1341–1346.
7. Foley, J.A., Asner, G.P., Costa, M.H., Coe, M.T., DeFries, R., Gibbs, H.K., Howard, E.A., Olson, S., Patz, J., Ramankutty, N. and others. Amazonia revealed: forest degradation and loss of ecosystem goods and services in the Amazon Basin. *Frontiers in Ecology and the Environment* **2007** vol. 5, n.1, 25–32.
8. Pires, G.F., Costa, M.H. Deforestation causes different subregional effects on the Amazon bioclimatic equilibrium. *Geophysical Research Letters* **2013** vol. 40, n.14, 3618–3623.
9. Garcia-Carreras, L., Parker, D.J. How does local tropical deforestation affect rainfall?. *Geophysical Research Letters* **2013** vol. 38, n.19.
10. D'Almeida, C., Vorosmarty, C.J., Hurtt, G.C., Marengo, J.A., Dingman, S.L., Keim, B.D. The effects of deforestation on the hydrological cycle in Amazonia: a review on scale and resolution. *International Journal of Climatology* **2007** vol. 27, n.5, 633–647.
11. Heckenberger, M.J., Russell, J.C., Toney, J.R., Schmidt, M.J. The legacy of cultural landscapes in the Brazilian Amazon: implications for biodiversity. *Philosophical Transactions of the Royal Society of London B: Biological Sciences* **2013** vol.362, n.1478, 197–208.
12. Malhi, Y., Roberts, J.T., Betts, R.A., Killeen, T.J., Li, W., Nobre, C.A. Climate change, deforestation, and the fate of the Amazon. *Science* **2013** vol.319, n.5860, 169–172.
13. Marengo, J.A. Long-term trends and cycles in the hydrometeorology of the Amazon basin since the late 1920s. *Hydrological Processes* **2009** vol.23, n.22, 3236–3244.
14. Saleska, S.R., Miller, S.D., Matross, D.M., Goulden, M.L., Wofsy, S.C., Da Rocha, H.R., De Camargo, P.B., Crill, P., Daube, B.C., De Freitas, H.C., others. Carbon in Amazon forests: unexpected seasonal fluxes and disturbance-induced losses. *Science* **2003** vol.302, n.5650, 1554–1557.
15. Poorter, L., Bongers, F., Aide, T.M., Zambrano, A.M.A., Balvanera, P., Becknell, J.M., Boukili, V., Brancalion, P.H.S., Broadbent, E.N., Chazdon, R.L. and others. Biomass resilience of Neotropical secondary forests. *Nature* **2016** vol. 530, n.7589, 211–214.
16. Winemiller, K.O., McIntyre, P.B., Castello, L., Fluet-Chouinard, E., Giarrizzo, T., Nam, S., Baird, I.G., Darwall, W., Lujan, N.K., Harrison, I. and others. Balancing hydropower and biodiversity in the Amazon, Congo, and Mekong. *Science* **2016** vol.351, n.6269, 128–129.
17. da Silva Soito, J.L., Freitas, M.A.V. Amazon and the expansion of hydropower in Brazil: Vulnerability, impacts and possibilities for adaptation to global climate change. *Renewable and Sustainable Energy Reviews* **2011** vol.15, n.6, 3165–3177.
18. Moore, R., Hancher, M., Thau, D. High-Resolution Global Maps of 21st-Century Forest Cover Change.
19. Morton, D.C., DeFries, R.S., Shimabukuro, Y.E., Anderson, L.O., Arai, E., del Bon Espirito-Santo, F., Freitas, R., Morisette, J. Cropland expansion changes deforestation dynamics in the southern Brazilian Amazon. *Proceedings of the National Academy of Sciences* **2006** vol. 103, n.39, 14637–14641.

Preprints (www.preprints.org) | NOT PEER-REVIEWED | Posted: 9 October 2023 doi:10.20944/preprints202310.0383.v1

20. Foley, J.A., DeFries, R., Asner, G.P., Barford, C., Bonan, G., Carpenter, S.R. Chapin, F.S., Coe, M.T., Daily, G.C., Gibbs, H.K. and others. Global consequences of land use. *Science* **2005** vol.309, n.5734, 570–574.
21. Nobre, A.D. O futuro climatico da Amazonia. *Relatorio de avaliacao cientifica* **2014** vol.31.
22. Poschl, U., Martin, S.T., Sinha, B., Chen, Q., Gunthe, S.S., Huffman, J.A., Borrmann, S., Farmer, D.K., Garland, R.M., Helas, G. and others. Rainforest aerosols as biogenic nuclei of clouds and precipitation in the Amazon.*Science* **2010** vol.329, n.5998, 1513–1516.
23. Mu, Q., Heinsch, F.A., Zhao, M., Running, S.W. Development of a global evapotranspiration algorithm based on MODIS and global meteorology data. *Remote sensing of Environment* **2007** vol.111, n.4, 519–536.
24. Filgueiras, E.T., Ribeiro, C.B.M. Estimativa de parâmetros d balanço hídico por base de dados de satélite na bacia hidrográfica do rio Amazonas. *XVI Simpósio de Recursos Hídricos do Nordeste e 15º Simpósio de Hidráulica e Recursos Hídricos dos Países de Língua Portuguesa* **2022**.
25. Nepstad, D., McGrath, D., Stickler, C., Alencar, A., Azevedo, A., Swette, B., Bezerra, T., DiGiano, M., Shimada, J., da Motta, R.S. and others. Slowing Amazon deforestation through public policy and interventions in beef and soy supply chains. *Science* **2014** vol.344, n.6188, 1118–1123..
26. Zarin, D.J. Legacy of fire slows carbon accumulation on amazonian forest regrowth. *Frontiers in Ecology and the Environment3 (7)* **2005** p 365-369.
27. Davidson, E.,A. Recuperation of nitrogen cycling in amazonian forests following agricultural abandonment. *Nature 447(7147)* **2007** p 995/998.
28. Pfaff, A., S., et al. Road impacts in brasillian amazonia. *Amazonia and global change* **2009** pp 101-106.
29. Pfaff, A., S., et al. What drives deflorestation in the brasilian amazon?: Evidence from satellite and socieconomic data. *Journal of Environmental Economics and Management* **1999** 37(1):26-43.
30. PArima, E., Y., Walker, R., T., Perz, S., G., Caldas, M. Loggers and forest fragmentation: Behavioral models of road building in the amazon basin. *Annals of the Association of American Geographers* **2005** 95(3):525-541.
31. PArima, E., Y., et al. The fragmentation of space in the amazon basin. *Photogrammetric Engineering & Remote Sensing* **2008** 74(6):699-709.
32. Walker, R., et al. Ranching and the new global range: Amazônia in the 21st century. *Geoforum* **2009** 40(5):732-745.
33. Nepstad, D., et al. Frontier governance in amazonia. *Science* **2002** 295(5555):629-631.
34. SOUZA Jr., Carlos M., SHIMBO, Julia Z., ROSA, Marcos R., PARENTE, Leandro L., ALENCAR, Ane A., RUDORFF, Bernardo F. T., HASENACK, Heinrich, MATSUMOTO, Marcelo, FERREIRA, Laerte G., SOUZA-FILHO, Pedro W. M., OLIVEIRA, Sergio W. de, ROCHA, Washington F., FONSECA, Antônio V., MARQUES, Camila B., DINIZ, Cesar G., COSTA, Diego, MONTEIRO, Dyeden, ROSA, Eduardo R., VÉLEZ-MARTIN, Eduardo, WEBER, Eliseu J., LENTI, Felipe E. B., PATERNOST, Fernando F., PAREYN, Frans G. C., SIQUEIRA, João V., VIERA, José L., FERREIRA NETO, Luiz C., SARAIVA, Marciano M., SALES, Marcio H., SALGADO, Moises P. G., VASCONCELOS, Rodrigo, GALANO, Soltan, MESQUITA, Vinicius V., AZEVEDO, Tasso. Reconstructing Three Decades of Land Use and Land Cover Changes in Brazilian Biomes with Landsat Archive and Earth Engine. *MDPI* **2020** v. 12, n. 17, p. 2735.
35. Llopart, M.,Reboita, M. S.,Coppola, E.,Giorgi, F.,da Rocha, R. P., de Souza, D. O. Land Use Change over the Amazon Forest and Its Impact on the Local Climate. *Water - MDPI* **2018**, 10(2), 182. https://doi.org/10.3390/w10020182
36. Nelva B. Riquetti, Samuel Beskow, Li Guo, Carlos R. Mello. Soil erosion assessment in the Amazon basin in the last 60 years of deforestation. *Environmental Research* **2023**,Vol 236 - Part 2, 116846, ISSN 0013-9351, https://doi.org/10.1016/j.envres.2023.116846.
37. Emmanuel Da Ponte, Fermín Alcasena, Tejas Bhagwat, Zhongyang Hu, Luca Eufemia, Ana Paula Dias Turetta, Michelle Bonatti, Stefan Sieber, Poppy-Louise Barr. Assessing wildfire activity and forest loss in protected areas of the Amazon basin. *Applied Geography* **2023**,Vol 157, 102970, ISSN 0143-6228, https://doi.org/10.1016/j.apgeog.2023.102970.
38. Santos, M. J., O'Connor, J. C., Nguyen, K., Tuinenburg, O., Dekker, S. C.Effects of land use change on water-related ecosystem services in the Amazon Basin. *EGU General Assembly* **2023**, EGU23-14983. https://doi.org/10.5194/egusphere-egu23-14983

Preprints (www.preprints.org) | NOT PEER-REVIEWED | Posted: 9 October 2023 doi:10.20944/preprints202310.0383.v1

39. Funk, Chris, Pete Peterson, Martin Landsfeld, Diego Pedreros, James Verdin, Shraddhanand Shukla, Gregory Husak, James Rowland, Laura Harrison, Andrew Hoell, Joel Michaelsen. The climate hazards infrared precipitation with stations-a new environmental record for monitoring extremes. *Scientific Data 2*, **2015** 150066, doi:10.1038/sdata.2015.66
40. Correndo, S., Mu, Q., Zhao, M.MODIS/Terra Net Evapotranspiration 8-Day L4 Global 500m SIN Grid V061. *distributed by NASA EOSDIS Land Processes Distributed Active Archive Center, https://doi.org/10.5067/MODIS/MOD16A2.061. Accessed 2023-09-12*, **2021** 150066,
41. da Rocha, N., S., Veettil, B., K., Grondona, A., E., B, Käfer, P., S., Iglesias, M., L., Diaz, L., R., Kaiser, E., A., da Silva, S., S., Rolim, S., B., A. IMPACTOS HIDROLÓGICOS NO RIO MADEIRA INFLUENCIADOS POR EVENTOS DE ENOS E ODP NAS GELEIRAS TROPICAIS ANDINAS *XIX Simpósio Brasileiro de Sensoriamento Remoto*, **2019**, 975-978, p. 4, ISBN 978-85-17-00097-3

Disclaimer/Publisher's Note: The statements, opinions and data contained in all publications are solely those of the individual author(s) and contributor(s) and not of MDPI and/or the editor(s). MDPI and/or the editor(s) disclaim responsibility for any injury to people or property resulting from any ideas, methods, instructions or products referred to in the content.